AD A109714

TECHNICAL REPORT ARBRL-TR-02382

HYDROCODE COMPUTATIONS AND EXPERIMENTAL INVESTIGATIONS OF EXPLOSIVE STAGED SHAPED CHARGE DEVICES

Fred I. Grace
Stanley K. Golaski
Brian R. Scott

DTIC
SELECT
JAN 1 8 1982
E

November 1981

US ARMY ARMAMENT RESEARCH AND DEVELOPMENT COMMAND
BALLISTIC RESEARCH LABORATORY
ABERDEEN PROVING GROUND, MARYLAND

01 18 82 029

REPORT DOCUMENTATION PAGE		READ INSTRUCTIONS BEFORE COMPLETING FORM
1 REPORT NUMBER TECHNICAL REPORT ARBRL-TR-02382	2. GOVT ACCESSION NO. AD-A109 714	3. RECIPIENT'S CATALOG NUMBER
4 TITLE *(and Subtitle)* HYDROCODE COMPUTATIONS AND EXPERIMENTAL INVESTIGATIONS OF EXPLOSIVE STAGED SHAPED CHARGE DEVICES.		5. TYPE OF REPORT & PERIOD COVERED Final
		6. PERFORMING ORG. REPORT NUMBER
7. AUTHOR(s) Fred I. Grace Stanley K. Golaski Brian R. Scott		8. CONTRACT OR GRANT NUMBER(s)
9. PERFORMING ORGANIZATION NAME AND ADDRESS US Ballistic Research Laboratory ATTN: DRDAR-BLT Aberdeen Proving Ground, MD 21005		10. PROGRAM ELEMENT, PROJECT, TASK AREA & WORK UNIT NUMBERS 1L1662618AH80
11. CONTROLLING OFFICE NAME AND ADDRESS US Army Armament Research & Development Command US Army Ballistic Research Laboratory ATTN: DRDAR-BL, APG, MD 21005		12. REPORT DATE NOVEMBER 1981
		13. NUMBER OF PAGES 32
14. MONITORING AGENCY NAME & ADDRESS*(If different from Controlling Office)*		15. SECURITY CLASS. *(of this report)* UNCLASSIFIED
		15a. DECLASSIFICATION/DOWNGRADING SCHEDULE
16 DISTRIBUTION STATEMENT *(of this Report)* Approved for public release, distribution unlimited.		
17. DISTRIBUTION STATEMENT *(of the abstract entered in Block 20, if different from Report)*		
18. SUPPLEMENTARY NOTES		
19. KEY WORDS *(Continue on reverse side if necessary and identify by block number)* Staged Shaped Charge Narrow Angle Liners Explosive Staging Technique Hydrocode (HEMP) Liner Collapse Calculations		

20. ABSTRACT *(Continue on reverse side if necessary and identify by block number)* (ael)

A staged shaped charge design is under investigation at the BRL. The device makes possible coherent shaped charge jets from extremely narrow angle liners. This is brought about through the explosive staging technique where the energy of the explosive is stored momentarily as kinetic energy of a metallic conical shell originally in contact with the high explosive, and then, delivered in a predetermined manner to an inner jetting metallic shaped charge liner. —> cont next page

DD FORM 1473 1 JAN 73 EDITION OF 1 NOV 65 IS OBSOLETE

Cont

20. The paper presents the physical design of the staged shaped charge and its principal of operation. The staging mechanism and liner collapse are described by both analytic and hydrocode approaches (HEMP). Experimental results are presented through radiographs flashed directly through the detonating charge showing the collapse process, jet formation, and early jet motion. These are compared directly with grid overlays calculated by HEMP. Results are presented for three inner liner materials; nickel, copper and aluminum.

TABLE OF CONTENTS

3

LIST OF FIGURES

5

INTRODUCTION

A shaped charge utilizes a metal lined conical cavity in an explosive and when detonated, its liner collapses on axis and forms a high velocity metallic jet which has the ability to penetrate deep into material targets. The collapse process and jet formation has been described by theory[1] which relates hydrodynamic flow to the geometry and certain physical properties of the explosive and metal. The parameters of importance include the explosive detonation velocity (D), liner collapse and flow velocities (V_ℓ and V_s), liner half angle α, metal throw-off angle (δ) and liner collapse angle (β). These are depicted in Figure 1.

It has been established that the liner flow velocity (V_s) into the stagnation region must not exceed the sound velocity for the metal under consideration in order to maintain subsonic flow and stable jetting. The diagram indicates that V_s can satisfy the subsonic flow condition when β is sufficiently large. For ideal explosives, β cannot be increased without limit through increases in δ, since δ is limited to 15°, typically. Thus, subsonic flow is achieved by proper choice of α, which in practice, is generally kept at or above 20°, (included angle of 40°). This lower practical limit for α can be traced ultimately to the high detonation rate of convential high energy military explosives and the relatively low sound velocity associated with medium dense metals such as copper, nickel and iron.[2] As a result, for a fixed angle cone, liner length, jet length and the corresponding penetration capability of the jet formed are limited by the device's diameter.

It is of interest to consider a cylindrical lined cavity shaped charge whose included angle (α) has been diminished to zero degrees. Some features of such a design are listed: (1) the jet length is independent of diameter but proportional to charge length, (2) for $\alpha=0$, the theory indicates $V_s = D$, (3) the jet velocity is two times the detonation rate and (4) the jet is steady state, although a velocity gradient can be designed into the system. Condition (2) above suggests a stable, coherent jet can be produced only under conditions where the explosive detonation rate and the sound velocity of the jetting cylinder are nearly equal.

---

1. E.M. Pugh, R.J. Eichelberger and N. Rostocker, "Theory of Jet Formation by Charges with Lined Conical Cavities", J. Appl. Phys., 23, 1952, p.p. 532-536.

2. M. van Thiel ed., Compendium of Shock Wave Data UCRL-50108, LRL, University of California, Livermore, June 1966.

7

$V_\ell = 2u \sin \delta$

$V_s = V_\ell \cos \tfrac{1}{2}(\beta + \alpha) \cdot \csc \beta$

$V_j = V_\ell (\csc \beta/2) \cos (\alpha/2)$
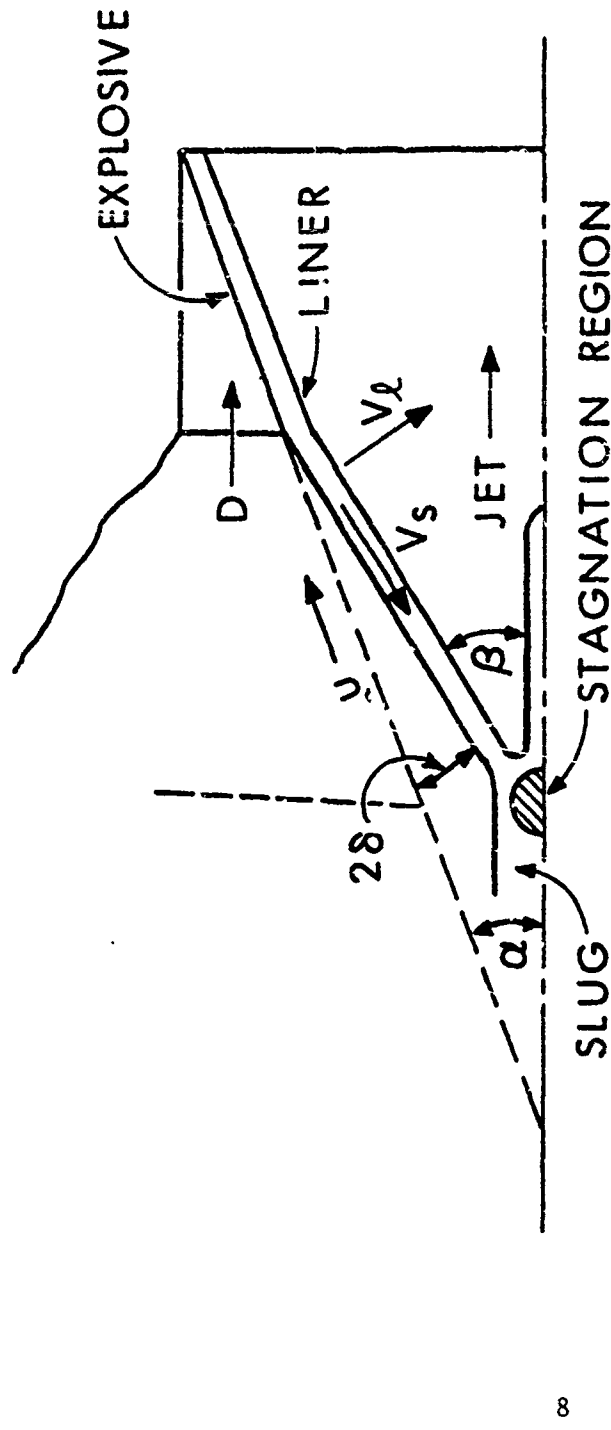
$V_s < C_0$ COHERENT JET (SUBSONIC)

$V_s > C_0$ INCOHERENT JET (SUPERSONIC)

$C_0 =$ LINER BULK SOUND VELOCITY

Figure 1. Schematic of shaped charge cone collapse.

Previous attempts,[3][4] have been made to jet metallic cylinders for explosive metal combinations which approach the above condition. These included Baratol/Aluminum (4.87 km/s / 5.35 km/s) and Composition B/Beryllium (7.84 km/s / 7.98 km/s). Although some success was reported with respect to jet coherency, low density metallic jets do not possess high penetration potential and systems with small collapse angles (β) do not possess massive jets. These difficulties and a lack of attractive explosive/metal combinations have prohibited practical designs for cylindrical shaped charges in the past.

In the present work, explosive staging[5] was utilized to produce an explosive driver system whose propagation rate along the liner was substantially lower than the explosive detonation velocity. We examined several possible designs which utilized conventional high energy explosives and traditional liner materials in near cylindrical geometries. Descriptions and results of the staged shaped charge are reported in the following sections.

I. PRINCIPLE OF OPERATION

A cross section of a staged shaped charge is shown in Figure 2. The device consists of an outside section of high explosives (1) in contact with a metal shell acting as a driver (2), space (or ambient air) (3,6), and a section of high explosive (4) which is in contact with the shaped charge metal liner (5). A detonator (7) initiates both sections of explosives (1) and (4). It is not necessary for both explosives to be initiated simultaneously, but for the purpose of describing the device function we assume that any difference is small. The detonation begins at the left and travels toward the right at a rate of about 8 km/s typically for conventional explosives.

---

3. *S. Kronman, unpublished work BRL.*

4. *S. Kronman and J. H. Kineke Jr., "Explosive Devices for Projecting Hypervelocity Pellets up to 21.0 km/sec." Proc. 5th Hypervelocity Symposium, Vol II, Nonr-(G)-0200-62(x), Colorado School of Mines, April 1962.*

5. *F. I. Grace, "Staged Shaped Charge", U.S. Patent # 4,187,782 , 12 Feb. 1980.*

1 EXPLOSIVE
2 METAL DRIVER CONE
3 VOID
4 EXPLOSIVE
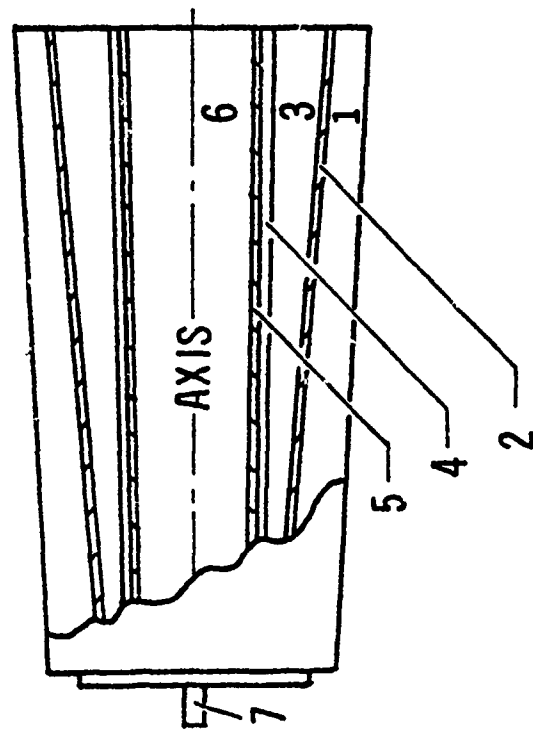5 METAL SHAPED CHARGE LINER
6 VOID
7 DETONATOR

Figure 2. Longitudinal section of staged shaped charge.

10

The energy of the main explosive charge (1) is imparted to the driver
(2), first at the initiated end (left) and to successive driver regions
in time from left to right. The driver (2) implodes on the gases
produced by the detonating inner explosive section (4). The implosion
of the driver (2) on the gaseous section transmits shocks through the
gas and accelerates the metal liner (5) toward the axis of the charge.
The velocity of the impact point is refered to as the phase velocity of
the device. The process which takes place can be visualized in
Figure 3.

For a conventional shaped charge the main explosive is in direct
contact with the metal liner. Therefore, the sweep rate (phase velocity)
of the acceleration pulse is the detonation velocity. In the staged
shaped charge, the phase velocity is controlled by the geometry of the
outer explosive and driver and the detonation velocity. The choice
of dimensions permits the phase velocity to be substantially less than
the detonation velocity. Therefore, the liner can be forced to bend
through a greater angle (δ) than is possible in the conventional
design. A larger bend angle (δ) permits the use of a lower initial
cone half angle (α) to achieve the same collapse angle (β).

II. SOLUTION RELATED TO DEVICE FUNCTION

In Figure 4a, a short section of the driver and liner are considered.
The liner makes an angle α with the axis and α^* with the driver. The
initiation of both explosive sections begins at point 0 and proceeds
to points A and A' in time t'. At this point the driver is accelerated
instantaneously to a velocity v_1 by force of the main (outer) explosive
section while the liner is accelerated to a lesser velocity v_3 by the
inner explosive section. At some later time t_3 the driver overtakes
the liner at point A" and delivers an impulsive acceleration to the
liner upon impact (neglect the thickness of the gas which actually
transfers the momentum between the two met . sections). A similar
phenomena occurs at point B when the detonation front reaches that
position at time t_2. However, at point B a lesser velocity V_2 is
imparted to the driver ($v_2 < v_1$) since the charge to mass (C/M)
ratio is purposely designed to get smaller in a continuous fashion
toward the base of the charge. At some later time t_4, the driver section
originally at point B overtakes the corresponding liner section at
point B", and upon impact accelerates the liner to a velocity V_3 also.
The time required for driver/liner impact is calculated at both
positions A and B. t=0 is taken when the detonation fronts reach the
position A-A'. The impact regions are shown in more detail in Figure
4b. At position A-A' the required time t_A is given by;

11

1 EXPLOSIVE
2 METAL DRIVER CONE
3 VOID
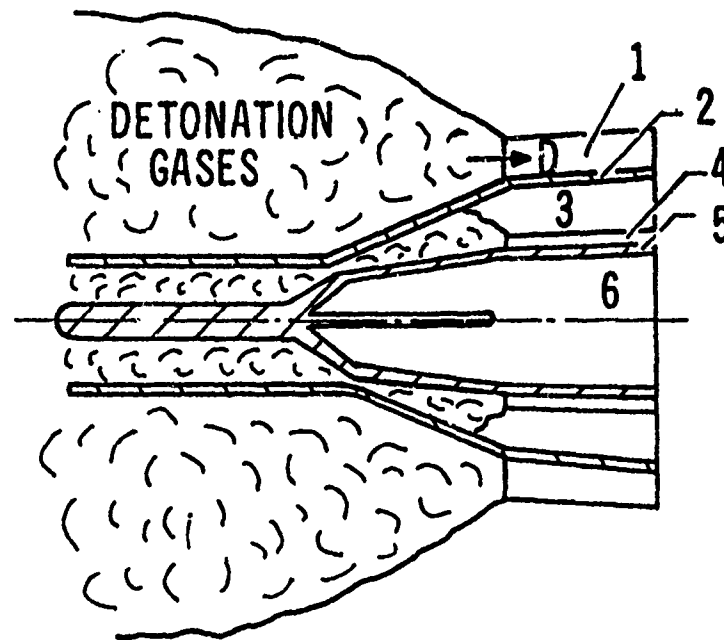4 EXPLOSIVE
5 METAL SHAPED CHARGE LINER
6 VOID

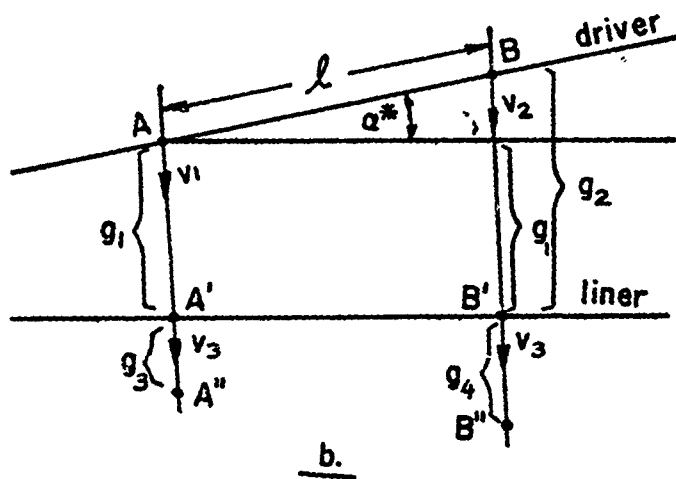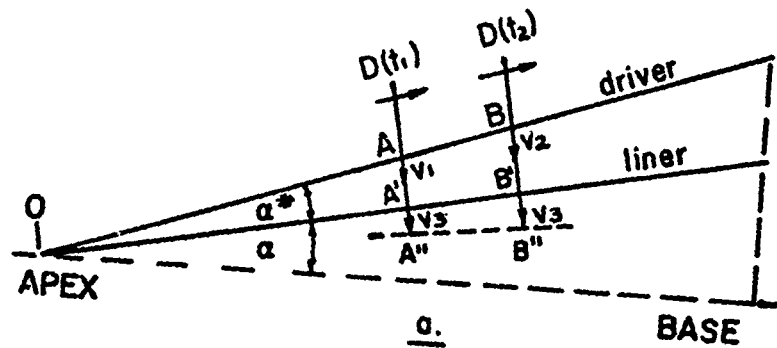Figure 3. Schematic of staged shaped charge
liner collapse.

Figure 4a & b.   Notation for computation of
staged shaped charge collapse.

13

$$t_A = \frac{g_1}{v_1} + \frac{g_3}{v_1} \text{ and also } t_A = \frac{g_3}{v_3}.$$

Thus

$$g_3 = g_1\left(\frac{v_3}{v_1 - v_3}\right) \text{ and } t_A = \frac{g_1}{v_1 - v_3} \qquad (1)$$

At position B-B' the impact occurs at t_B.

$$t_B = \frac{\ell}{D} + t_C \text{ or } t_B = \frac{\ell}{D} + \frac{g_2}{v_2} + \frac{g_4}{v_2}$$

where $\frac{\ell}{D}$ is just the time required for the detonation fronts to pass from points A-A' to B-B'.

Also $\qquad t_C = \frac{g_4}{v_3}$ which gives $g_4 = g_2\left(\frac{v_3}{v_2 - v_3}\right)$.

Thus

$$t_B = \frac{\ell}{D} + \frac{g_2}{v_2 - v_3} \qquad (2)$$

The difference in time for the impact point to travel between two positions A" and B" is denoted t and is given by the difference between equations (2) and (1)

$$t = \frac{\ell}{D} + \frac{g_2}{v_2 - v_3} - \frac{g_1}{v_1 - v_3}$$

The phase velocity $v_p = \ell/t$ is given by

$$V_p = \frac{\ell}{\frac{\ell}{D} + \frac{g_2}{v_2 - v_3} - \frac{g_1}{v_1 - v_3}} \qquad (3)$$

It is believed that the final liner velocity (v_3) after driver/ liner impact is at least as high as the liner collapse velocity (v_ℓ) produced by a conventional charge. This is based upon previous results[6] which show that the staged system can be more efficient and that even higher velocities can be obtained for a given total C/M for the system. The liner velocity typically would equal 2 km/s. When typical values are substituted into equation (3), a phase velocity as low as 4 km/s is possible.

---

6. H. Sternberg and D. Piacasi, "Explosion Hydrodynamic Calculations for a Two-Staged Guided Missile Warhead", NOL TR 63-72, Feb 63.

III. HYDROCODE APPROACH

The algebraic relations used up to this point approximate the characteristics of interest during the collapse process. However, this simplified formulation fails to model two or three dimensional effects that occur in most real applications. The HEMP[7] computer program was used for a fuller description since it contains the essential features. It has been successfully applied to similar shaped charge problems at this facility, and its accuracy and limitations are familiar.

The HEMP code can treat time-dependent, two dimensional, multi-material problems involving large deformations and high deformation rates. It numerically solves the system of partial differential equations for the conservation of mass, momentum and energy, with appropriate initial and boundary conditions. An explicit, Lagrangian, finite difference scheme is utilized. Both hydrodynamic and elastic-perfectly plastic material models are included and an energy release routine simulates the detonation of high explosive materials. Figure 5 shows typical computational grids for the staged shaped charge; one for the initial conditions and the other for the solution at 32 microseconds.

Various boundary conditions were applied at the left initiation surface. The rigid wall condition was found to be the most reasonable approximation to the experimental configuration (neglecting the explosive head and inert plug). Free surfaces were assumed for the remaining exterior boundaries of the grid. The explosive materials were modeled with a J.W.L. form equation of state. The region between the driver cone and the inner explosive was filled with air modeled with an ideal gas equation of state. A frictionless slide surface was allowed between the outer explosive and the driver cone, preventing large shear type distortions that would otherwise develop in the expanding explosive by-products. No such slide surface was implemented between the liner and the inner explosive since it was assumed that far less expansion could occur due to the confinement of the driver.

The deformed grid reflects the calculation of the staged implosion at 32 microseconds after explosive initiation. At this time the detonation has traveled the majority of the explosive length and both the driver and liner have been accelerated towards the axis of symmetry.

---

7. Mark L. Wilkins, "Calculation of Elastic and Plastic Flow",
    UCRL-7322, LRL, University of California, Rev I, 1969.

15
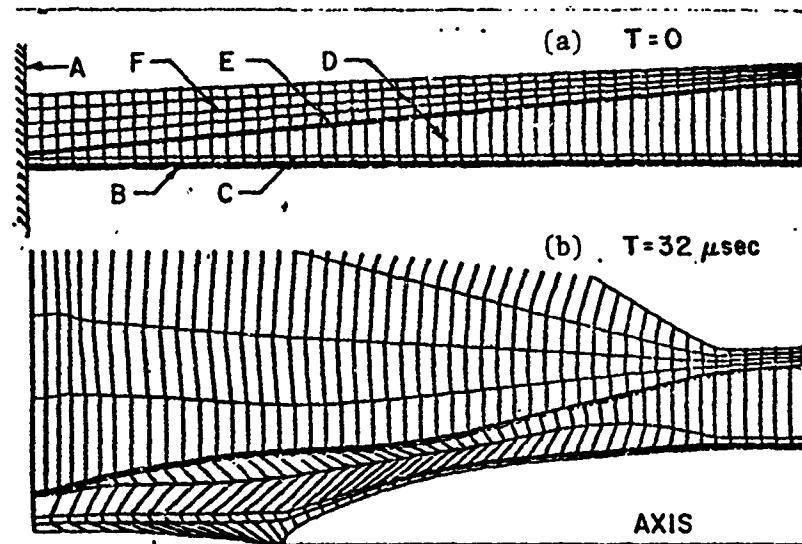
A= Rigid Boundary and Initiation Surface
B= Metal Liner
C= Liner Explosive
D= Void
E= Metal Driver
F= Driver Explosive

Figure 5. HEMP GRID (a) t=0, (b) t= 32μs.

Two cells were allotted across the liner thickness, reducing large distortions associated with jetting. Throughout the calculation as each liner element approached the axis, the flow properties given by HEMP were recorded for later use as input to the 1-D, steady state, incompressible jet formation theory[1]. In this way, estimations for the axial jet velocity distribution and the liner displacement field in the stagnation region were obtained. The geometries of the liner, driver, inner and outer explosives were parametrically varied within design constraints in order to produce optimum jet characteristics. In addition, the effect of initiation scheme, confinement, alternate materials, etc. could be investigated. Such calculations were used to establish experimental designs.

IV. EXPERIMENTAL DESIGN AND RESULTS

HEMP calculations were made for a number of staged designs using various explosives, liner materials and inner cylinders. Designs were selected for further study on the basis of calculated values for the flow velocity into the stagnation region and the collapse angle β. The HEMP calculations indicated that for the cylindrical inner liner configuration it was possible to achieve subsonic flow into the stagnation region if the driver explosive had a detonation velocity on the order of 6 km/s. To achieve subsonic flow with Composition B (D=7.84 km/s) a conical inner liner (albeit a relatively small α was required, at least for the higher density, low sound velocity metals.

To verify the staged shaped charge concept, the design shown in Figure 6 was chosen. The device was fabricated with a copper conical inner liner having a 30° included angle. The driver system consisted of a Composition B main charge, 42° included angle copper driver and 2mm thick inner explosive of DuPont Detasheet. The device was conservative (relatively large α), since the intention was to verify the staging action and to produce a jet. The HEMP calculations predicted a subsonic collapse throughout with reasonable β angles. Figure 7 is a photograph of the 600 Kv radiograph taken 46 µsec after initiation of the charge. The staging action between the driver and the inner liner can easily be seen along with the resulting jet. The experiment thus verified the concept of the staged shaped charge. The appearance of the coherent jet indicates a subsonic collapse. The collapse angles were very close to those predicted by HEMP. Futher, it is to be noted that the staging did not introduce any undo perturbations into the system. Further experiments were conducted with the staged design shown in Figure 8. The design employed a liner with a 17° included angle and a driver cone with a 27° included angle. The main explosive was Composition B and the inner explosive
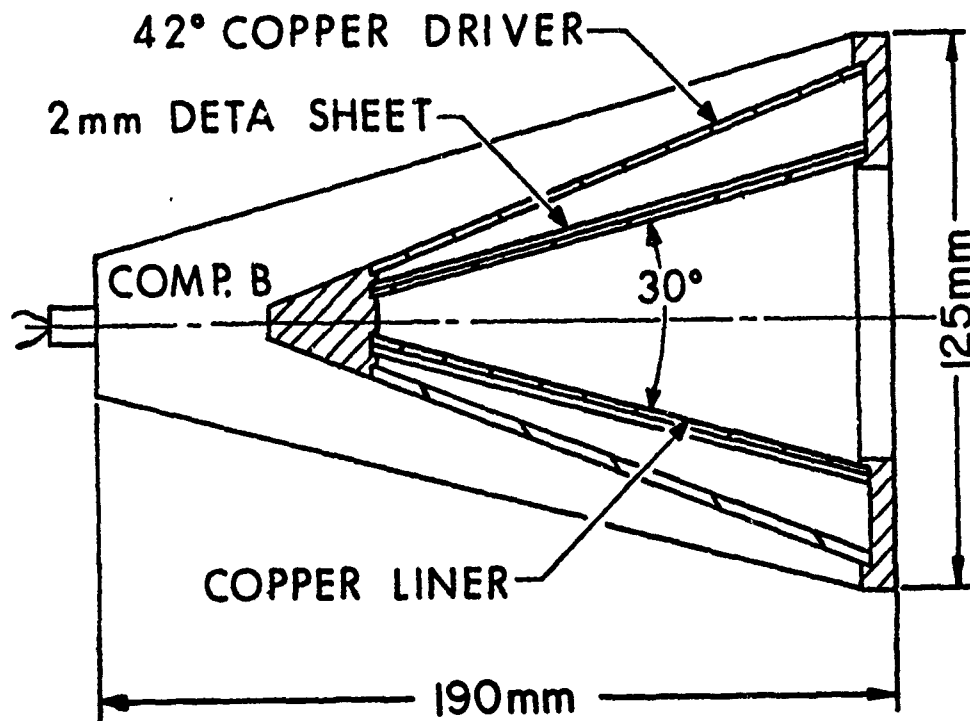
17

Figure 6. 30° x 42° staged shaped charge design.

25mm

Figure 7. Radiograph of 30° x 42° staged shaped charge
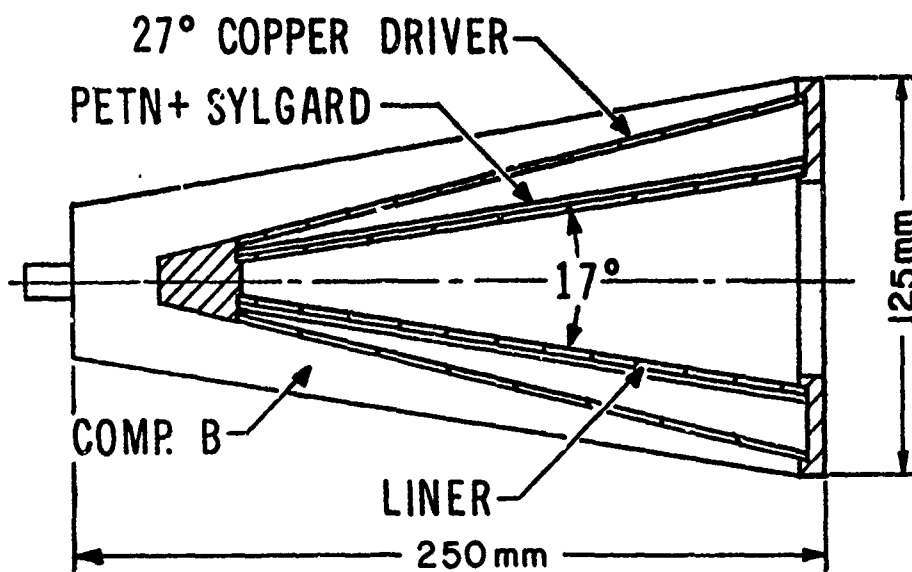46μs after initiation.

Figure 8. 17° x 27° staged shaped charge design.

20

of 2mm thickness was an extrudable explosive consisting of 80% PETN and 20% Sylgard.

Three liner materials were investigated: (1) Oxygen Free High Conductivity Copper (OFHC), (2) Electroformed Nickel, (3) 1100 F Aluminum. Figure 9 is a plot of the expected flow velocity as a function of axial position. It can be noted that the nickel and aluminum designs were subsonic throughout the collapse sequence while the copper design begins with a supersonic collapse near the apex, but successive elements along the axis were subsonic.

Figures 10, 11 and 12 show radiographs of the above designs wherein nickel and aluminum liners have produced coherent jets. The copper lined design produced a jet with a bifurcated supersonic leading portion and a coherent subsequent portion, however the coherent portion displayed relatively early breakup. Figure 11 shows the collapse of the aluminum staged charge at 23.8 µs after the start of staging and a HEMP grid at approximately the same time. The start of staging is the initiation of driver collapse. The agreement is seen to be excellent.

As stated earlier, the computations indicated that it was possible to achieve subsonic flow for collapsing cylindrical liners (or nearly cylindrical) if the explosive used in the driver system has a detonation velocity of approximately 6 km/s. An aluminum lined staged device was built with a zero degree liner and employed EL 506 (D=7.0 km/s) as the driver explosive. Also a staged device using a 4° included angle nickel 270 liner and TNT (D=7.0 km/s) as the driver explosive was built and tested. Both charges produced coherent but wavy jets. Table I summarizes the staged shaped charge results to date.

From the table it can be seen that staging can be employed to produce jets from narrow angle liners. It can also be seen that the theoretical predictions for phase velocity, collapse angle and jet tip velocity are very close to the experimental results. This indicates that the HEMP + 1-D theory calculations are sufficiently accurate to design relatively complicated shaped charge devices. The present experiments and analyses suggest that explosive staging may not be able to produce coherent jets from cylindrical systems of copper or other metals of interest, which have a low sound velocity, particularily when high energy military explosives are utilized. However, any developments in high energy explosives with intermediate detonation rates (5-6 km/s) could be combined with explosive staging to produce successful cylindrical shaped charge designs.

21

TABLE I

| SUMMARY OF STAGED SHAPED CHARGE RESULTS									
STAGED DEVICE	EXPLOSIVE	PHASE VELOCITY km/s		COLLAPSE ANGLE degrees		JET TIP VELOCITY km/s		JET QUALITY	
		THEORY	EXPT.	THEORY	EXPT.	THEORY	EXPT.	1CD	15CD
30° LINER Cu	COMP B	3.6	3.1	38	35	6.7	6.4	COHERENT	COHERENT BUT EARLY BREAKUP
17° LINER Cu	COMP B	4.8	4.6	26	25	7.85	7.6	INCOHERENT	REAR COHERENT BUT EARLY BREAKUP
Ni	COMP B	4.8	4.6	26	–	7.85	7.8	COHERENT	COHERENT
..	COMP B	4.8	4.9	26	28	9.7	8.8	COHERENT	COHERENT
4° LINER Ni	TNT	–	–	24	20	–	–	COHERENT BUT WAVY	
0° LINER Al	EL-506C	–	–	24	22.5	–	–	COHERENT	
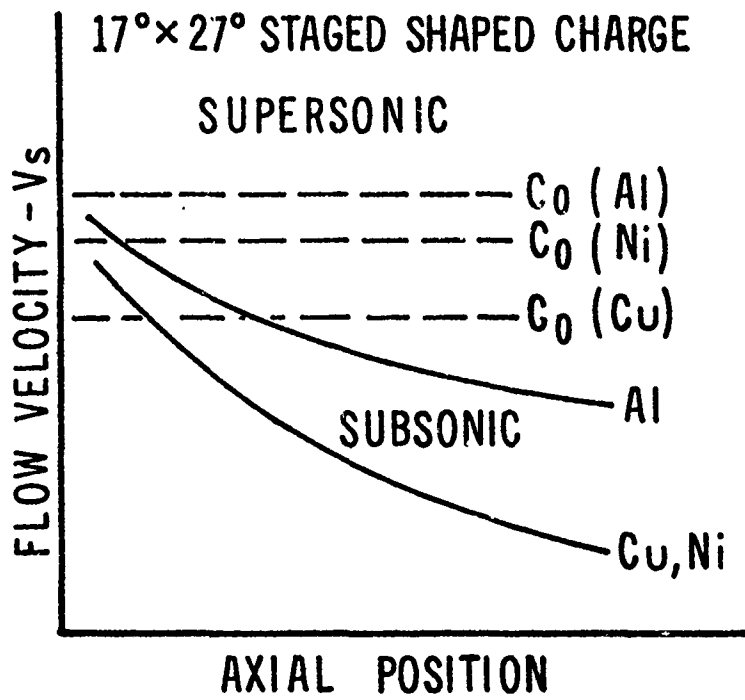
Figure 9. Flow velocity vs axial position
          for 17° x 27° staged shaped charge.
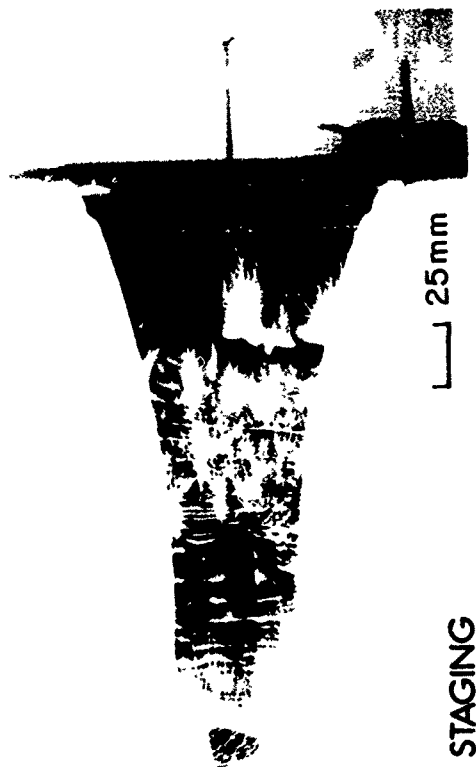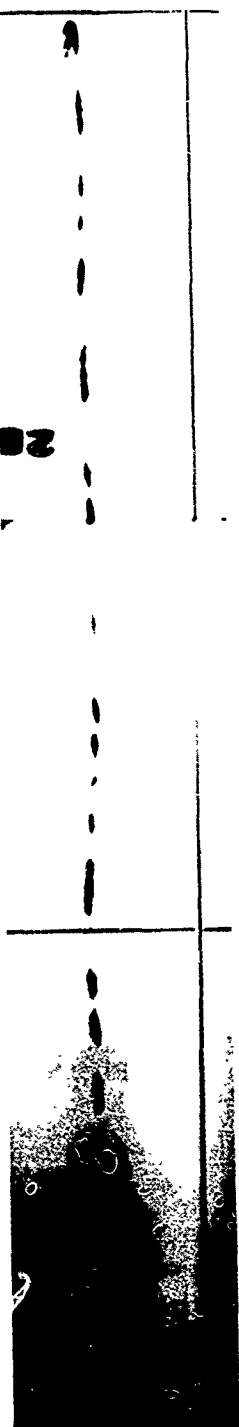
t₁ = 40 μs AFTER STAGING

t₂ = 165 μs AFTER STAGING
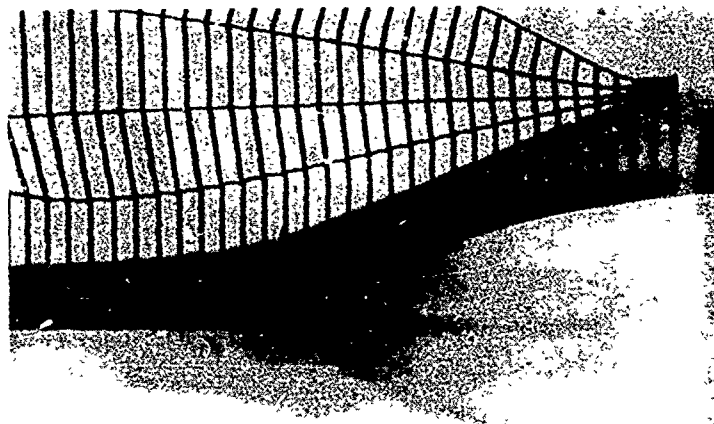
Figure 10. Radiograph of 17° x 27° nickel staged shaped charge. $t_1 = 40 \mu s$, $t_2 = 165 \mu s$ after staging.

L_____J 25mm

Figure 11. Radiograph of 17° x 27° aluminum
staged snaped charge with HEMP GRID
overlay. t= 23.8µs after staging.
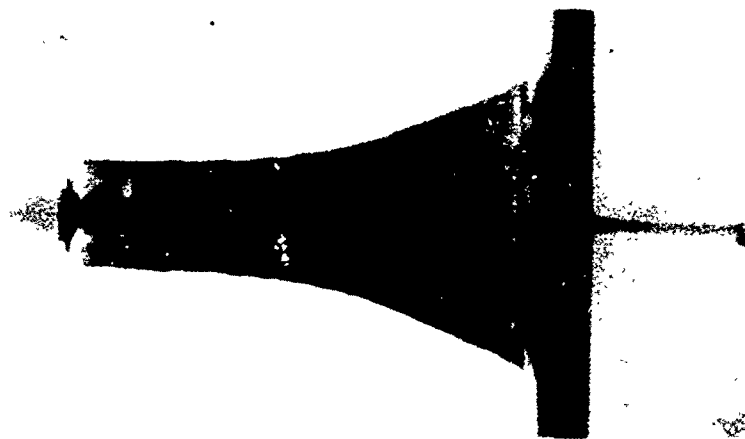
L__J 25mm

Figure 12. Radiograph of 17° x 27° aluminum
          staged shaped charge. t= 36.6μs after staging.

V. CONCLUSIONS

The conclusions which may be drawn from the staging experiments conducted to date are as follows:

Staging action has been verified. Coherent jets have been obtained from low angle devices in aluminum and nickel.

The phase velocity, acting upon the inner cylinder, has been significantly reduced below the detonation velocity of the high explosive driving the system. Reductions as low as 50 to 60 percent of the detonation velocity are possible.

Higher than normal metal throw off angles are achieved with resulting high collapse angles (β).

HEMP serves as a useful diagnostic tool in determining viable designs.

DISTRIBUTION LIST

No. of Copies	Organization	No. of Copies	Organization
12	Commander Defense Technical Info Center ATTN: DDC-DDA Cameron Station Alexandria, VA 22314	1	Commander US Army Armament Materiel Readiness Command ATTN: DRSAR-LEP-L, Tech Lib Rock Island, IL 61299
1	Deputy Under Secretary of the Army (Operations Research) ATTN: SAUS-OR, D.C. Hardison Room 2E621, The Pentagon Washington, DC 20310	1	Director US Army ARRADCOM Benet Weapons Laboratory ATTN: DRDAR-LCB-TL Watervliet, NY 12189
1	Assistant Secretary of The Army (R&D) ATTN: Asst.for Research Washington, DC 20310	1	Commander US Army Aviation Research and Development Command ATTN: DRDAV-E 4300 Goodfellow Boulevard St. Louis, MO 63120
2	HQDA (DAMA-ZA; DAMA-RA, T. Rorstad) Washington, DC 20310	1	Director US Army Air Mobility Research and Development Laboratory Ames Research Center Moffett Field, CA 94035
1	Commander US Army Materiel Development and Readiness Command ATTN: DRCDMD-ST 5001 Eisenhower Avenue Alexandria, VA 22333		
1	Commander US Army Materiel Development and Readiness Command ATTN: DRCCG 5001 Eisenhower Avenue Alexandria, VA 22333	1	Commander US Army Communications Rsch and Development Command ATTN: DRDCO-PPA-SA Fort Monmouth, NJ 07703
1	Commander US Army Materiel Development and Readiness Command ATTN: DRCDE-WM 5001 Eisenhower Avenue Alexandria, VA 22333	1	Commander US Army Electronics Research and Development Command Technical Support Activity ATTN: DELSD-L Fort Monmouth, NJ 07703
		1	Commander US Army Missile Command ATTN: DRSMI-VIT Redstone Arsenal, AL 35809
5	Commander US Army Armament Research and Development Command ATTN: DRDAR-TSS (2 cys) DRDAR-LCU-D-R, T. Stevens DRDAR-LCU-LT, A. King DRDAR-LCU-DC, J. Pearson Dover, NJ 07801	1	Commander US Army Missile Command ATTN: DRSMI-XB, M. Yoakum Redstone Arsenal, AL 35809

29

DISTRIBUTION LIST

No. of Copies	Organization	No. of Copies	Organization
1	Commander US Army Missile Command ATTN: DRSMI-R Redstone Arsenal, AL 35809	2	Commander US Army Materials and Mechanics Research Center ATTN: DRXMR-PDD, J. Prifti Tech Lib Watertown, MA 02172
1	Commander US Army Missile Command ATTN: DRSMI-J COL C.M. Matthews, Jr. Redstone Arsenal, AL 35809	1	Commander US Army Research Office P. O. Box 12211 Research Triangle Park, NC 27709
2	Commander US Army Missile Command ATTN: DRCPM-HFE, COL Cass R. Masucci Redstone Arsenal, AL 35809	1	Director US Army TRADOC Systems Analysis Activity ATTN: ATAA-SL, Tech Lib White Sands Missile Range NM 88002
1	Commander US Army Missile Command ATTN: DRCPM-DT Redstone Arsenal, AL 35809	2	Chief of Naval Research Department of the Navy ATTN: Code 427 Code 470 Washington, DC 20360
1	Commander US Army Missile Command ATTN: DRSMI-YDL Redstone Arsenal, AL 35809	2	Commander Naval Air Systems Command ATTN: Code AIR-310 Code AIR-350 Washington, DC 20360
1	Commander US Army Missile Command ATTN: TOW-PM, COL Williamson Redstone Arsenal, AL 35809		
3	Commander US Army Tank Automotive Research and Development Command ATTN: DRDTA-RWL, C. Bradley DRDTA-UL DRDTA-RC, Dr. J. Jellinek Warren, MI 48090	4	Commander Naval Surface Weapons Center ATTN: Code DG-50 DX-21, Lib Br. Dr. W. Soper Mr. C. Cooper Dahlgren, VA 22448
1	Project Manager, XM1 Tank Sys ATTN: Mr. J. Roossien 28150 Dequindre Warren, MI 48090	3	Commander Naval Surface Weapons Center ATTN: Code 730, Lib Mr. N. Colebarn Dr. J. Foltz Silver Spring, MD 20910

30

DISTRIBUTION LIST

No. of Copies	Organization	No. of Copies	Organization
3	Commander Naval Weapons Center ATTN: Code 3835 Code 3431, Tech Lib Dr. L. Smith China Lake, CA 93555	1	Director Lawrence Livermore National Lab ATTN: Dr. C. Godfrey P. O. Box 808 Livermore, CA 94550
1	Commander Naval Research Laboratory Washington, DC 20375	1	Director Lawrence Livermore National Lab ATTN: Dr. R. Jandrisevits P. O. Box 808 Livermore, CA 94550
1	USAF/AFRDDA Washington, DC 20311	1	Director Los Alamos National Laboratory ATTN: Dr. W. Mautz Los Alamos, NM 87544
1	AFSC/SDZ Andrews AFB Washington, DC 20311		
2	US Air Force Academy ATTN: Code FJS-41 (NC) Tech Lib Colorado Springs, CO 80840	1	AFELM, The Rand Corporation ATTN: Library-D 1700 Main Street Santa Monica, CA 90406
1	AFATL/DLJR (J. Foster) Eglin AFB, FL 32542	1	Battelle-Columbus Laboratories ATTN: Mr. Joseph E. Backofen 505 King Avenue Columbus, OH 43201
1	AFATL/DLYV (Mr. J. Smith) Eglin AFB, FL 32542	1	Dyna East Corporation ATTN: P. C. Chou 227 Hemlock Road Wynnewood, PA 19096
1	AFWL/SUL (LT Tennant) Kirtland AFB, NM 87116		
1	AFAL/WR Wright-Patterson AFB, OH 45433	2	Firestone Defense Research and Products Division of the Firestone Tire and Rubber Company ATTN: R. Berus L. Swabley 1200 Firestone Parkway Akron, OH 44317
1	AFLC/MMWMC Wright-Patterson AFB, OH 45433		
1	Director Lawrence Livermore National Lab ATTN: Tech Lib P. O. Box 808 Livermore, CA 94550	1	Honeywell, Inc. Government and Aeronautical Products Division ATTN: C. R. Hargreaves 600 Second Street, NE Hopkins, MN 55343
1	Director Lawrence Livermore National Lab ATTN: Dr. J. Kury P. O. Box 808 Livermore, CA 94550		

DISTRIBUTION LIST